sciendo

*ASN, Vol 6, No1, Pages 63-72,* 2019

**Acta Scientifica Naturalis**
Former Annual of Konstantin Preslavsky University – Chemistry, Physics, Biology, Geography
Journal homepage: asn.shu.bg

Received: 03.2019
Accepted: 04.2019

# Comparative Study of the Bacteriological Activity of Zinc Oxide and Copper Oxide Nanoparticles

Abdelali Merah[1], Abdenabi Abidi[2], Hana Merad[1], Noureddine Gherraf[3], Mostepha Iezid[4], Abdelghani Djahoudi[5]

[1] *Laboratory of Mineral Chemistry, Department of Pharmacy, Faculty of Medicine, Annaba, Algeria*

[2] *Laboratory of Organic Synthesis, Modeling and Optimization of Chemical Processes Department of Process Engineering, University of Badji-Mokhtar, Annaba 23000, Algeria*

[3] *Laboratory of Natural Resources and Management of Sensitive Environments; Larbi Ben M'hidi University, Oum El Bouaghi 04000, Algeria*

[4] *Laboratoire d'Innovation en construction, Eco-conception et Génie Sismique (LICEGS); Université Mostafa Ben Boulaid Batna 2, 05000, Algeria*
[5] *Laboratory of Microbiology, Department of Pharmacy, Faculty of Medicine, University of Badji-Mokhtar, Annaba, 23000, Algeria*

**Abstract :** *Interest in nanomaterials, especially metal oxides, in the fight against resistant and constantly changing bacterial strains, is more and more expressed. Their very high reactivity, resulting from their large surface area, promoted them to the rank of potential successors of antibiotics.*

*Our work consisted of the synthesis of zinc oxide (ZnO) and copper oxide (CuO) in the nanoparticle state and the study of their bactericidal effect on various Gram-negative and Gram-positive bacterial strains.*

*The nanoparticles of metal oxides have been synthesized by sol-gel method. Qualitative analysis and characterization by UV / Visible and infrared spectrophotometry and X-ray diffraction confirmed that the synthetic products are crystalline. The application of the Scherrer equation allows to determine the size of the two metal oxides, namely: 76.94 nm for ZnO and 24.86 nm for CuO.*

*The bactericidal effect of ZnO and CuO nanoparticles was tested on Gram-positive bacteria (Staphylococcus aureus, Staphylococcus hominis, Staphylococcus haemolyticus, Enterococcus facials) and Gram-negative bacteria (Escherichia coli, Schigella, Klepsiella pneumoniae and Pseudomonas aeruginosa). The results indicate that the tested metal oxides nanoparticles have an effect that varies depending on bacterial species. Indeed, Gram-positive bacteria show greater sensitivity to ZnO nanoparticles whereas Gram-negative bacteria are more sensitive to CuO nanoparticles.*

**Key words:** Nanoparticles, ZnO, CuO, sol-gel method, bactericidal effect

## Introduction

The development of nano-biotechnology today offers tiny tools, whose exceptional properties make it possible to consider cutting-edge applications in pharmacy and biomedicine. Work aims to


*Corresponding author:* abidi1ml @yahoo.com
DOI: 10.2478/asn-2019-0009 

develop safer treatments with the possibility of therapeutic targeting or biocompatible surfaces for implants and orthopedic devices, nanoparticle-based adjuvant vaccines and antibacterial nano-particulate agents.

The "sol-gel" process is therefore generally used to prepare metal oxides by hydrolysis of metal precursors, generally alkoxides in alcohol solution or metal salts in aqueous solution. The condensation of the hydroxide molecules formed, by elimination of water, leads to the formation of a network. Gelation is achieved and a porous and dense gel is obtained. Solvent removal by drying allows the formation of an ultrafine metal hydroxide powder network. A heat treatment of the hydroxide leads to the corresponding metal oxide. The rate of hydrolysis and condensation are important parameters that affect the properties of the final product. Slow and controlled hydrolysis generally results in smaller particle sizes [1-3]

A study carried out by Nejati et al [4] on the elaboration of zinc oxide nanoparticles showed that the addition of the $KNO_3$ and $K_2SO_4$ and $LiNO_3$ reagents to the process as well as by modifying the molar ratio at different values could alter the size and morphology of synthesized nanoparticles. Sharma et al. [5] worked on the synthesis of zinc oxide nanoparticles by the sol-gel method and the bactericidal effect, and showed that these nanoparticles exhibit a bactericidal activity on *E. Coli*. MTCC 40 using the disk diffusion method. The study performed by Azam et al. [6] on the effect of nanoparticle size of copper oxide on antimicrobial activity on some Gram positive and Gram negative strains showed that antimicrobial activity of Copper oxide nanoparticles correlated well with the size of these nanomaterials.

In fact, the reduction of the size of the copper and zinc oxides in the nanoparticulate state, allows them to acquire new physicochemical properties among which the power to penetrate inside the bacteria and the immune cells and thus by biochemical mechanisms to disrupt their metabolisms: either by freeing the destruction of bacteria or releases of promising pro-inflammatory molecules for their cytotoxic effect [6].

In addition, in vivo and in vitro pulmonary inhalation studies showed that exposure to ZnO nanoparticles induces production of a variety of pro-inflammatory cytokines, TNF-α, IFN-γ and IL-12 [7]. Another study showed the influence of the size of ZnO nanoparticles on the release of cytokines from immune cells [8]. Moreover, it was reported that by exposing human aortic endothelial cells (H.A.E.C) to nanoparticles induces an inflammatory response which would depend on their compositions [9].
Another study by Beyerie et al [10] consisted to develop nanoscale inhalation drug delivery systems based on Zinc oxide nanoparticles, tested on alveolar epithelial cells led to the conclusion, that these nanoparticles caused a higher toxicity which is correlated with their higher surface area. Similarly, a previous study demonstrated that the use of nanoparticles could one day explain at the molecular level the immune responses induced during pathological processes related to cancer [11]. Finally, thanks to nanotechnologies, the immune responses of the human body to cancer attacks are well understood [12].

**Material and methods**

The equipment used is simple, consisting of a Sartorius brand analytical balance (BP 310 P); a magnetic stirrer heater (IKA MAG RET); an oven (KOTERMANN 2712); Muffle furnace (RAPA TRADE, ELECTRIC FURNACE zedxsz²HM-2) and Wattman filters.

For the synthesis of ZnO nanoparticles, the reagents used are: zinc acetate [Zn $(CH_3COOH)_2$. $2H_2O$] delivered by the supplier Merck and oxalic acid ($C_2H_2O_4$ .$2H_20$) delivered by Fluka.
The zinc oxide nanoparticles were prepared by the sol-gel method according to the protocol below: a 0.01M solution of zinc acetate is introduced into a beaker and kept stirring, then added with a 0.03M oxalic acid solution. At the end of the reaction we obtain a white suspension which is left standing for 18 hours in the reaction medium (maturation stage).

After filtration we obtain a white gel, which is washed three times with distilled water. The washed gel is then dried in the oven at 100 ° C for four hours. The product obtained is calcined at 600 °C.


*Corresponding author:* abidi1ml @yahoo.com
DOI: 10.2478/asn-2019-0009 

At the end of this step, the product is collected, finely ground and kept in sterile containers and protected from light.

For the synthesis of CuO copper oxide nanoparticles, the reagents used are: copper nitrate dihydrate delivered by Chemopharma; citric acid delivered by Fluka. The material used is the same for the synthesis of zinc oxide.

The nanoparticles of copper oxide were prepared by the sol-gel method according to the protocol: a 0.5M solution of copper nitrate is introduced into a beaker and kept stirring at a temperature of 100 ° C, and then added dropwise 0.5M of citric acid solution. Stirring is maintained for four hours at 100 °C.
At the end of the reaction, we obtain a blue-colored gel, which blackened after being heated to 200 ° C on the heating stirrer. The fluffy mass obtained in black color is then calcined in the muffle furnace at 600 ° C for one hour. The collected product is finely ground and stored in sterile containers and protected from light.

**Results and discussions:**

The spectral screening was performed by a JASCO model V-530 UV-visible spectrophotometer between (200 and 700 nm). As support, we used Quartz tanks with an optical path of one cm.

- **zinc oxide powder**

The spectrum obtained shows (FIG. 1): a maximum of absorbance at 374 nm. solid zinc oxide is characterized by a peak of absorbance at 380 nm; the difference between these two values can be attributed to the "blushift" bluing phenomenon defined by a decrease in the frequency of the electromagnetic waves. This phenomenon represents the expression of the electronic confinement characteristic of nanostructures.

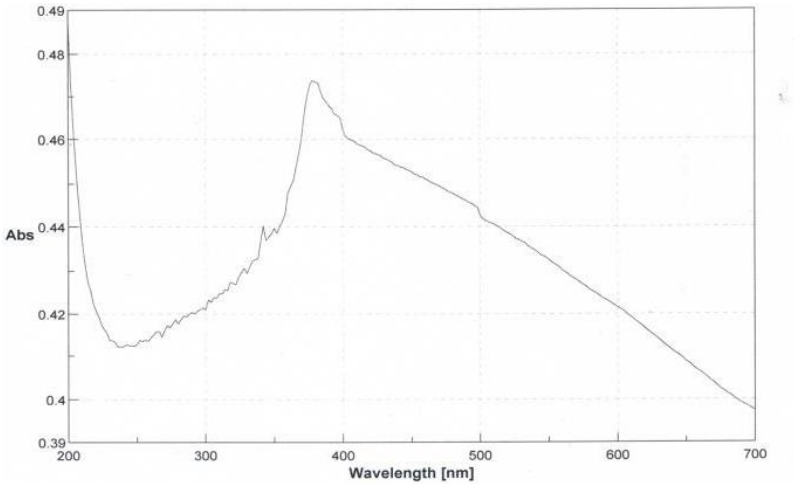


**Fig.1:** UV-Visible spectrum of nanostructures of ZnO

- **copper oxide powder**

The UV-visible spectrum shows (FIG. 2) a maximum absorbance at 350 nm which, compared to that of a solid copper oxide, would indicate the same phenomenon of bluing. As for the ZnO powder, the electronic confinement of the CuO particles directs us towards a nanoparticle structure of the synthesized products.


*Corresponding author:* abidi1ml @yahoo.com
DOI: 10.2478/asn-2019-0009 

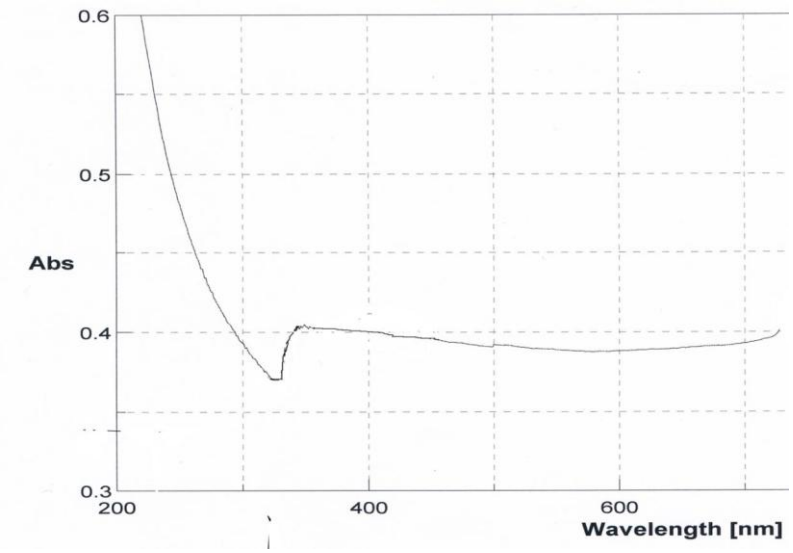


**Fig.2:** UV-Visible spectrum of nanostructures of CuO

**Characterization by infrared spectroscopy:**

The apparatus used is a Brunker-Alpha brand Fourier Transform Infrared Spectrophotometer, the area of interest extends from (400-4000 cm -1) with a resolution of 2 $cm^{-1}$.

- **zinc oxide powder**

The spectrum (FIG. 3) has a main absorption band at 443 $cm^{-1}$ attributed to the Zn-O vibrations characteristic of the metal-oxygen bond (M-O). Moreover, the band observed at 1635 can be attributed to the angular deformation of water H-OH, while the band appeared at 3422 $cm^{-1}$ can be attributed to the elongation vibration O-H of water. The infrared spectrum confirms that the synthesized powder corresponds to the metal oxide (ZnO). The intensity of the absorbance tells us about the presence of traces of impurities (bands 1635, 3422 cm-1) which correspond to traces of water probably coming from the ambient humidity. Moreover, these results are in agreement with the values reported in the literature [6].

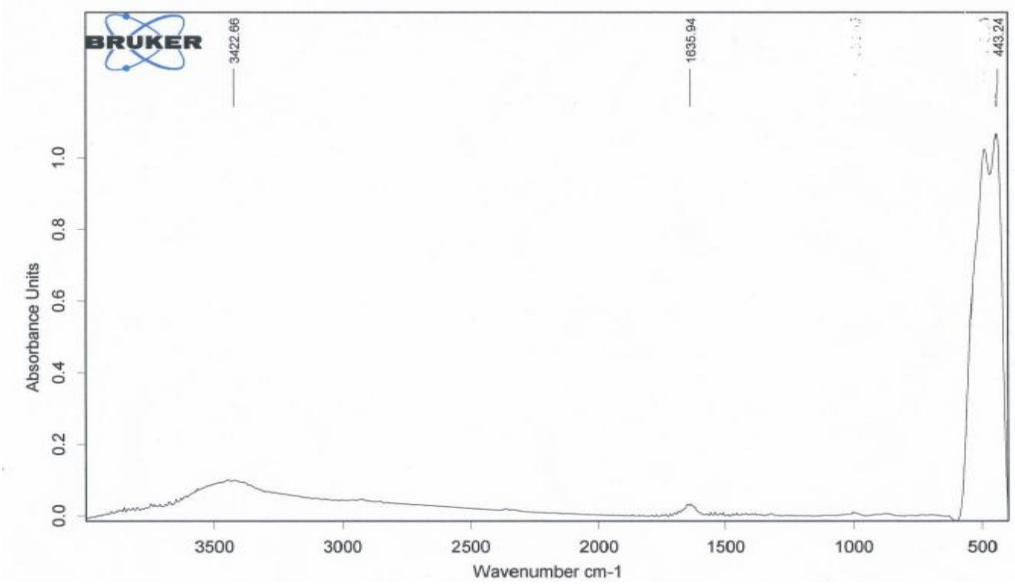


**Fig. 3**: IR spectrum of the synthesized zinc oxide



*Corresponding author:* abidi1ml @yahoo.com

DOI: 10.2478/asn-2019-0009 

- **copper oxide powder**

The spectrum (Fig. 4) shows a main absorption band at 531 cm $^{-1}$ attributed to Cu-O vibrations. In addition, the band observed at 1631 cm$^{-1}$ can be attributed to the angular deformation of H-OH water. The band appeared at 2923 cm$^{-1}$ could be attributed to $CO_2$ vibrations; while the band at 3418 corresponds to the O-H elongation vibration of the water. The infrared spectrum confirms that the synthesized powder corresponds to CuO. As for ZnO powder, the intensity of the absorbance tells us about the presence of traces of impurities (bands 1631, 3418 cm$^{-1}$) which correspond to traces of water probably coming from the ambient humidity. Contamination of the sample with atmospheric $CO_2$ is believed to be responsible for the 2923 cm$^{-1}$ band.

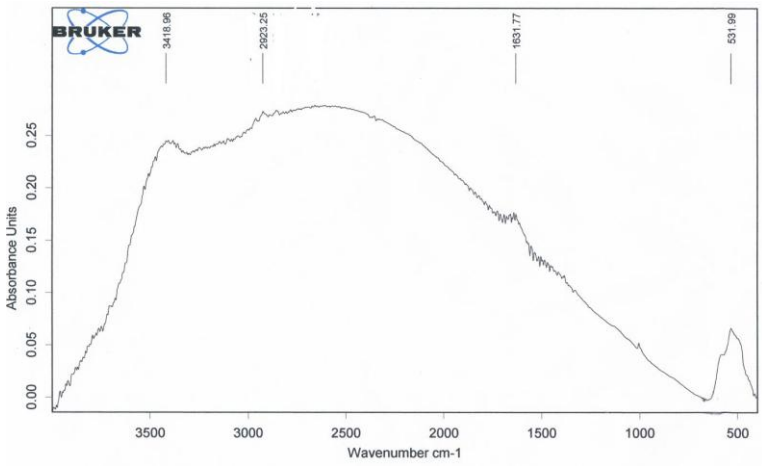


**Fig.4:** IR spectrum of the synthesized copper oxide

**Characterization by X-ray diffraction:**

The crystal structure and the size of the nanostructures were determined by the Brugg Brestan Analytical Xpert X-ray diffractometer with Cu- Kα radiation, a wavelength λ = 0. 15406nm and a two theta interval (30- 80 °).

- **zinc oxide powder:**

The zinc oxide diffraction diagram is shown in Fig. 5. We observe well resolved and intense peaks, located at the positions. 2θ: 31.84-34.52-36.33-47.63- 56.71-62.96-66.31-68.13-69.18-72.63-77.03. According to the Joint Committee on Powder Diffraction Standards (JCPDS) sheet No. 36-1451 for zinc oxide, these peaks correspond to the hexagonal Wurtzite phase (group P63mc). Moreover, no peak of impurities is observable in the limit of detection of the apparatus. The material is therefore of satisfactory purity. The diffraction diagram is consistent with that found for ZnO nanoparticles (Fig.7) according to Azam et al [6].


*Corresponding author:* abidi1ml @yahoo.com
DOI: 10.2478/asn-2019-0009 

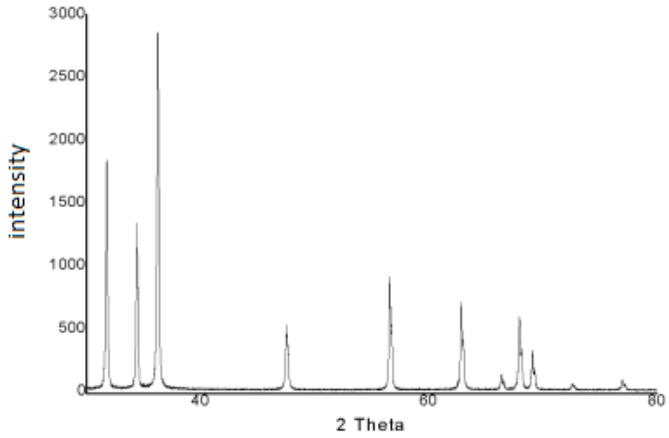


**Fig.5:** diagram DRX of nanostructures powder of ZnO

- **copper oxide powder:**

The X-ray diffraction diagram of copper oxide is presented on Fig. 6. We observe well-defined and intense diffraction peaks located at the positions:
2θ = 33.40-36.12-38.25-49.33- 54.63-58.84-61.69-65.60-66.01-68.22. According to Copper Oxide Data Sheet (JCPDS) No. 80-1916, these peaks correspond to the monoclinic structure of CuO. As for ZnO, no peak of impurities is observable in the detection limit of the device. The material is therefore of satisfactory purity. The diffraction spectrum is confirmed to that of the copper oxide nanoparticles (Fig. 7) according to Azam et al [6].

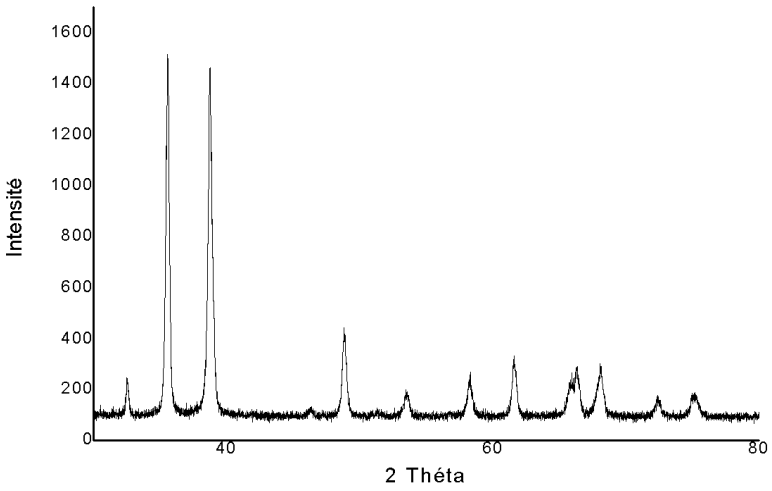


**Fig.6:** diagram DRX of nanostructures powder of CuO


*Corresponding author:* abidi1ml @yahoo.com
DOI: 10.2478/asn-2019-0009 

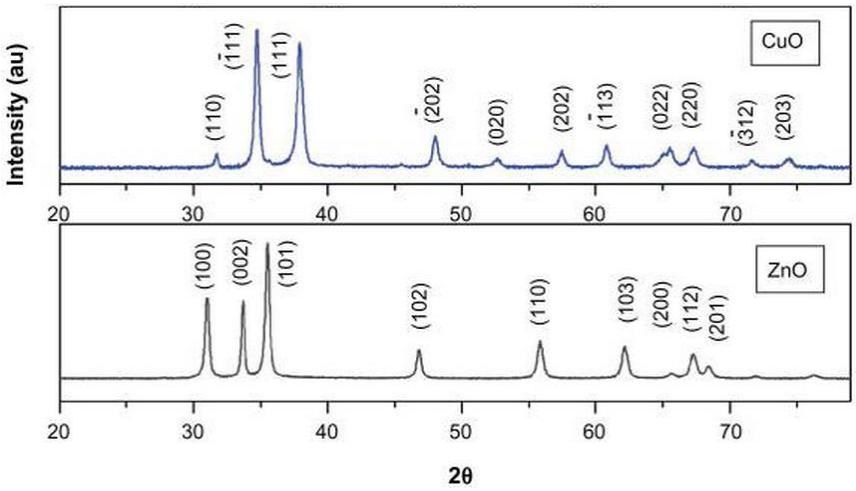


**Fig.7:** reference spectra of the nanoparticles of CuO and ZnO

**Calculation of the ZnO and CuO particle diameter**

Scherrer's relationship allows to calculate the particle diameter by exploiting the data delivered by the X-ray diffraction spectra [13,14].

$D = 0.9\ \lambda / \beta\cos\theta$

D: diameter of the nanoparticles expressed in (nm)

λ: wavelength of X-rays

β: width at mid-height of the most intense peak measured by diffraction expressed in radians

θ: the Bragg diffraction angle of the peak expressed in degree

Table -1. Below, contains all the data relating to ZnO and CuO particles. Applying Scherrer's formula, the diameters of the ZnO and CuO particles are respectively 76.94 nm and 24.86 nm.

**Table.1:** Data of x-rays diffraction

| **Oxide** | **λ (nm)** | **θ (°)** | **β (°)** | **β (radian)** |
|---|---|---|---|---|
| ZnO | 0.15405 | 36.33 | 0.081 | 0.001396 |
| CuO | 0.15405 | 36.12 | 0.225 | 0.003927 |

**Antibacterial activity of ZnO and CuO nanoparticles:**

This is a qualitative technique for determining the sensitivity of microorganisms to a known anti-microbial substance. This method relies on the migratory power of the substance inside a petri dish, in a solid nutrient medium (Mueller-Hinton). A one-milliliter inoculum is seeded on the surface of Muller-Hinton medium previously cast in petri dishes. When the agar becomes dry, the sterile disks (6mm in diameter) impregnated with nanostructures of ZnO and CuO stock solutions (1000 µg / L) and four dilutions will be deposited in the boxes. These are then closed and left for 15 minutes, the time required for diffusion, and then incubated at 37 ° C for 24 hours. After incubation, the absence of bacterial growth, expressing antimicrobial activity, results in a translucent halo around the disc, having the same color as the sterile agar and whose diameter (expressed in mm) is measured using a caliper. Negative control disks are prepared by placing them on agar inoculated nanopowders. The sensitivity of different strains to metal oxide nanostructures is classified as follows:

Not sensitive (-): inhibition diameter less than or equal to 6mm
Sensitive (+): inhibition diameter between 7 and 14mm
Very sensitive (++): inhibition diameter between 15 and 19mm
Extremely sensitive (+++): inhibition diameter greater than or equal to 20mm


*Corresponding author:* abidi1ml @yahoo.com
DOI: 10.2478/asn-2019-0009 

We note that there is a correlation between the diameter of the zone of inhibition and the minimum inhibitory concentration. The greater the zone of inhibition, the lower the concentration of the antibacterial agent required to inhibit the bacterial growth of the organisms. Hereinafter, Tables (2) and (3) which show the diameters of the zones of inhibition for ZnO and CuO nanoparticles:

**Table.2:** Diameters of inhibition zones for ZnO nanostructures

| | **strain** | **[ZnO] in µg/mL** | | | | |
|---|---|---|---|---|---|---|
| | | 1000 | 500 | 250 | 125 | 65 |
| Gram positive Bacteria | *Staphylococcus hominis* | 13.1 | 12.4 | 14.2 | 16.1 | <6 |
| | *Staphylococcus haemolyticus* | <6 | <6 | <6 | 14.4 | <6 |
| | *Staphylococcus aureus S47* | 9.2 | 11.7 | 17.6 | 18.1 | 18.8 |
| | *Staphylococcus aureus ATCC* | 19.1 | 18.2 | 15.3 | 15.6 | 19.3 |
| | *Enterococcus feacatis S118* | 9.5 | 12.3 | 16.3 | 18.6 | 19.4 |
| Gram negative Bacteria | *Escherichia Coli S53* | <6 | <6 | <6 | <6 | <6 |
| | *Schigella sp* | <6 | <6 | <6 | <6 | <6 |
| | *Klepsiella pneumonae* | <6 | <6 | 14.2 | 18.3 | <6 |
| | *Pseudomonas aeuroginosa* | 16.2 | 16.9 | 16.7 | 15.1 | 9.4 |

**Table.3:** Diameters of the inhibition zones for CuO nanostructures

| | strain | **[CuO] in µg/mL** | | | | |
|---|---|---|---|---|---|---|
| | | 1000 | 500 | 250 | 125 | 65 |
| Gram positive Bacteria | *Staphylococcus hominis* | <6 | 16.2 | <6 | <6 | <6 |
| | *Staphylococcus haemolyticus* | <6 | <6 | <6 | <6 | <6 |
| | *Staphylococcus aureus S47* | <6 | <6 | <6 | 13.1 | 14.2 |
| | *Staphylococcus aureus ATCC* | <6 | <6 | <6 | <6 | 11.3 |
| | *Enterococcus feacatis S118* | 18.2 | 19.1 | 18.8 | 16.8 | 15.1 |
| Gram negative Bacteria | *Escherichia Coli S53* | 16.2 | 17.7 | 16.6 | 14.2 | 11.2 |
| | *Schigella sp* | 11.4 | 15.2 | 16.2 | 18.1 | 16.1 |
| | *Klepsiella pneumonae* | <6 | <6 | <6 | <6 | <6 |
| | *Pseudomonas aeuroginosa* | 9.4 | 9.1 | 11.2 | 15.2 | 17.4 |

The results indicate that ZnO and CuO metal oxide nanoparticles do indeed have a bactericidal effect on both Gram-positive and Gram-negative strains. The bactericidal effect seems to extend also on strains of *Pseudomonas aeuroginosa* and *Staphylococcus aureus* particularly known for their multidrug resistance. This effect is more pronounced in zinc oxide nanoparticles. The influence of the concentration on the size of the inhibition diameter remains however mixed. While it appears that the bactericidal effect is proportional to the concentration on strains such as *Enterococcus feacalis* S118 and *Escherichia coli* S53 with CuO and *Pseudomonas aeuroginosa* with ZnO, it shows an opposite trend in *Enterococcus feacalis* S118 and *Staphylococcus aureus* S47 with ZnO and *Schigella* sp and *Pseudomonas aeuroginosa* with CuO.

We also note that zinc oxide nanoparticles have a stronger antibacterial effect on Gram-positive strains while copper oxide shows greater efficacy on Gram-negative strains. This would be explained a



*Corresponding author:* abidi1ml @yahoo.com

DOI: 10.2478/asn-2019-0009 

priori by the difference in size between the two nanoparticles, but also by the properties of $Zn^{2+}$ and $Cu^{2+}$ cations. Further study on the mechanisms of action of the two oxides on bacterial strains is necessary to elucidate this point.

**Conclusion**

The aim of this work was to test the antibacterial effect of zinc oxide and copper oxide nanoparticles on Gram positive and Gram negative bacterial strains. At first, a batch of each oxide was synthesized at our laboratory level by "sol-gel" method. This method, both simple and inexpensive, led to the development of two batches of powders that we analyzed qualitatively and characterized by spectrophotometric methods UV / visible, infrared and X-ray diffraction.

The qualitative analysis of the two powders confirmed the presence of the $Zn^{2+}$ and $Cu^{2+}$ ion. Characterization by UV / Visible spectrophotometry indicated a blue shift phenomenon which would be the expression of the characteristic electronic confinement of the nanostructures. Infrared spectrophotometry revealed the existence of the metal-oxygen bond for the two products and made it possible to affirm that the synthesized powders correspond to the oxides of copper and zinc. X-ray diffraction allowed to establish the crystalline structure of the two metal oxides; a structure of Wurtzite type for ZnO and monoclinic for CuO. Finally, the application of the Scherrer equation allowed us to determine the size of the two metal oxides namely: 76.94 nm for ZnO and 24.86 nm for CuO.

Finally, the bactericidal effect of these two nanoparticles has been tested on various bacterial strains successfully. Both nanostructures have shown an antibacterial effect, especially on bacteria known as multi-resistant to antibiotics such as: *Pseudomonas aurogenosa, Klepsiella pneumonae* and *Staphylococcus aureus*. Gram-positive bacteria proved more sensitive to the action of ZnO nanostructures while Gram-negative bacteria were more sensitive to the action of CuO nanostructures.

To conclude, nanoparticles of ZnO and CuO appear to be a new tool for fighting bacteria, including those that show resistance to common antibiotics. They constitute not only a potential for the treatment of nosocomial infections but also, a preventive way in hospital environments, to use for example in aerosols to disinfect the premises or in ointment for the disinfection of the skin of the medical staff.

**References**:

[1] Hench, L.L.; West, J.K., The sol-gel process, *Chem. Rev*., **1990**, *90*, 33-72

[2] Wright, J. D.; Sommerdijk, N. A. J. M., Sol-gel materials: chemistry and applications. *Advanced chemistry texts*, **2001**, *4*. Amsterdam: Gordon and Breach Science Publishers.

[3] Brinker, C. J.; Scherer, G. W., Sol-Gel Science: Physics and Chemistry of Sol-Gel Processing *Academic Press*, **1990**

[4]. Nejati, A.; Rezvani, Z.; Pakizev, R., Synthesis of ZnO Nanoparticles and Investigation of the Ionic Template Effect on Their Size and Shape, *Int. Nano Lett*., **2011,** *1*(2), 75-81.

[5]. Sharma, V., Sol-Gel mediated facile synthesis of Zinc-Oxide nanoaggregates their characterization and antibacterial activity, *J.App. Chem*., **2012**, *6*, 52-55

[6]. Azam, A.; Ahmed, S.A.; Oves, M.; Khan, S.M.; Habib, S.S.; Memic, A., Antimicrobial activity of metal oxide nanoparticles against Gram-positive and Gram-negative: a comparative study, *Int. J. of Nanomedicine*, **2012**, *7*, 6003-6009

[7]. Sayes, C.M.; Reed, K.L.; Warheit, D.B., Assessing toxicity of fine and nanoparticles: comparing in vitro measurements to in vivo pulmonary toxicity profiles, *Toxicol. Sci*., **2007**, *97*(1), 163-180.

[8]. Hanley, C.; Thurber, A.; Hanna, C.; Punnoose, A.; Zhang, J.; Wingett, D.G., The Influences of Cell Type and ZnO Nanoparticle Size on Immune Cell Cytotoxicity and Cytokine Induction., *Nanoscale Res. Lett*., **2009**, *4*, 1409-1420.

[9]. Gojova, A.; Guo, B.; Kota, R.S.; Rutledge, J.C.; Kennedy, I.M.; Barakat, A.I., Induction of inflammation in vascular endothelial cells by metal oxide nanoparticles: effect of particle composition, *Environ. Health Perspect*., **2007**, *115*, 403-409.



*Corresponding author:* abidi1ml @yahoo.com

DOI: 10.2478/asn-2019-0009 

[10]. Beyerie, A.; Schulz, H.; Kissel, T.; Stoeger, T., Screening strategy to avoid toxicological hazards of inhaled nanoparticles for drug delivery: the use of alpha-quartz and nano-zinc oxide particles as benchmark, *Inhaled Particles*, **2009**, *151*, 1-9.
[11]Croft, M., The role of TNF superfamily members in T-cell function and diseases, *Nat. Rev. Immunol*., **2009**, *9*, 271-285.
[12] Lappin, M.B.; Campbell, J.D., The Th1-Th2 classification of cellular immune responses: concepts, current thinking and applications in hematological malignancy, *Blood Rev*., **2000**, *14*, 228-239.
[13] Scherrer, P*., Göttinger Nachrichten Gesell*., **1918**, *2*, 98
[14] Patterson, A., "The Scherrer Formula for X-Ray Particle Size Determination", *Phys. Rev*., **1939**, *56*(10), 978–982


*Corresponding author:* abidi1ml @yahoo.com
DOI: 10.2478/asn-2019-0009 